Pergamon

Wat. Sci. Tech. Vol. 29, No. 1–2, pp. 267–275, 1994.

0273–1223/94 $7·00 + 0·00

SIMULATION OF BASIN SCALE RUNOFF REDUCTION BY INFILTRATION SYSTEMS

S. Herath and K. Musiake

Department of Buildings and Civil Engineering, Institute of Industrial Science, University of Tokyo 7-22-1, Roppongi, Minato-ku, Tokyo 1606, Japan

ABSTRACT

A modelling approach is presented to simulate infiltration systems in urban areas. The model consists of a hydrological sub-model and an infiltration system sub-model. Infiltration characteristics of individual facilities are first established using steady state numerical simulation of Richards' equation. These are represented as linear relations between the facility water head and infiltration rate for given facility widths. The infiltration system model is obtained by applying continuity equation to infiltration facilities lumped over a sub-catchment. This model is then coupled to a catchment runoff model to simulate storm runoff with infiltration systems. The model is applied to an infiltration system installation in a residential area, where stormwater runoff is monitored in a pilot area and a comparative area. The observed results suggest the method is adequate to evaluate the performance of infiltration systems. Except for the catchment storage routing parameter, all model parameters are determined from physical catchment characteristics.

KEYWORDS

Infiltration; infiltration system modelling; catchment runoff; runoff reduction; soil hydraulic properties.

INTRODUCTION

World-wide urbanization creates new demands on urban drainage and flood control. This is due to the increases in runoff volumes as well as peak discharges which basically result from the loss of natural retention areas and expansion of impervious areas which prevent natural infiltration. To cope with increased storm runoff in receiving waters, various regulations have come into force in the recent past in rapidly urbanizing regions. One such requirement is that developers provide adequate retention facilities within the areas being developed. Here, infiltration systems can play an important role by reducing the extent of retention storage required. In Japan, infiltration systems consisting of infiltration trenches and collection boxes, which also act as filters, are popular and extensively used.

In order to ascertain the effectiveness of infiltration systems, it is necessary to estimate the reduction of storm water discharge by them at a scale representative of the areas being developed. Although infiltration from individual trenches can be estimated using Richards' equation (eg. Herath and Musiake, 1987), utilizing

such techniques at catchment scale requires large computational resources. Moreover such evaluations are needed in the planning stage, where simple models are attractive to carry out repetitive computations.

METHODOLOGY

Modelling Trench Infiltration Capacity

Infiltration capacity of a trench, for various water heads, can be estimated through numerical solution of Richards' equation, given by:

$$\nabla\cdot[k(\varphi)\nabla(\varphi-z)]=c(\varphi)\frac{\delta\varphi}{\delta t} \tag{1}$$

where φ = the soil water, $k(\varphi)$ = the soil conductivity, $c(\varphi) = \delta\theta/\delta\varphi$, and θ = moisture content.

The infiltration rate decreases with time and attains a final steady state due to the formation of a saturated "bulb" in the vicinity of the trench. This final infiltration capacity can be estimated more efficiently through numerical solution of the steady state of Richard's equation given by:

$$\nabla\cdot[k(\varphi)\nabla(\varphi-z)]=0 \tag{2}$$

By expressing the conductivity as a function of saturated conductivity and the relative conductivity ($kr(\varphi)$),

$$k(\varphi)=K_0 kr(\varphi) \tag{3}$$

it is possible to normalize eq.(2), with respect to saturated conductivity (K_0), which is the most sensitive soil parameter. The equation is then solved numerically using a finite difference scheme with fixed boundary conditions defined by the equations listed below and shown in Fig. 1.

$0 \le z \le z_n$, $x = x_n$	$\varphi = \varphi_n$ or $\delta\varphi/\delta x = 0$
$z = z_n$, $0 \le x \le x_n$	$\varphi = \varphi_n$
$z = 0$, $x > a$	$\varphi = \varphi_n$
$z = z_b$, $x \le a$	$\varphi = h$
$z_t \le z \le z_b$, $x = a$	$\varphi = z_b - z_t$
$0 \le z < z_b$, $x = a$	$\delta\varphi/\delta x = 0$
$z_b \le z \le z_n$, $x = 0$	$\delta\varphi/\delta x = 0$

where

z = depth measured vertically downwards from the surface
x = horizontal length starting from the trench centre line
z_b = the depth to trench bottom
z_t = the depth to trench top water level
z_n = model region extent in vertical direction
x_n = model region extent in horizontal direction
φ_n = fixed water pressure at field capacity
a = half width of the trench, and
h = water head within the trench ($= z_t - z_b$).

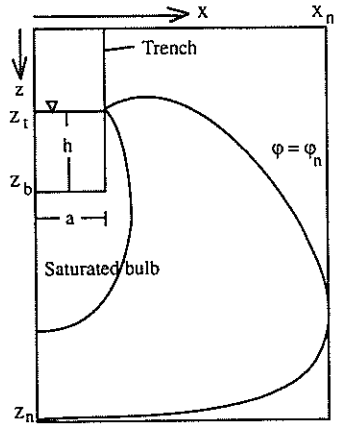

Fig. 1. Model domain used for numerical simulation

The details of an efficient numerical scheme with moving grids are discussed in Herath *et al*. (1992). Once the solution is obtained, Darcy's equation is used to compute infiltration rates from the facility. From a number of simulations corresponding to different water heads, normalized infiltration rate curves (q/K_0) for different trench dimensions can be established using eq.(4). Such a set of curves for Kanto Loam soil, a soil of volcanic ash origin commonly found in the Kanto area, Japan, is shown in Fig. 2.

$$\frac{q}{K_0} = \int_{x=0}^{x=a} |kr(\varphi) \frac{\delta(\varphi - z)}{\delta z}|_{z=z_t} dx + \int_{z=z_t}^{z=z_b} |kr(\varphi) \frac{\delta(\varphi)}{\delta x}|_{x=a} dz \tag{4}$$

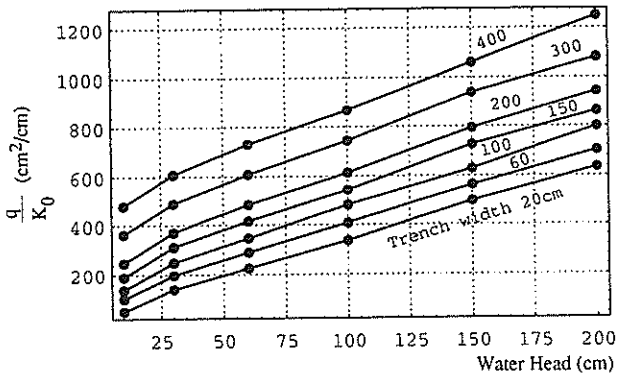

Fig. 2. q/K_0 vs. water head for infiltration trenches in Kanto Loam soils.

From the above figure it can be seen that for a limited range of water head within a trench of a given width, the trench water level (h) and infiltration (q) relationship can be represented by a linear equation of the form:

$$\frac{q}{K_0} = ah + b \tag{5}$$

The storage within the trenches also plays an important role in the storm discharge reduction. This is represented by the continuity equation for trench, expressed as,

$$\frac{dS}{dt}=i-qL=i-LK_0(ah+b) \tag{6}$$

where

L = the length of the trenches
S = trench storage
i = inflow to the trenches

Equations (5) and (6) together represent the dynamics of an infiltration system.

Catchment Runoff and Infiltration Systems

Various catchment models are available to the hydrologist to represent the transformation of rainfall into surface runoff. They vary from physically based distributed models to models representing hydrological processes lumped in different temporal and spatial scales, and to the rational formula and its modifications. In the design of urban storm drainage, the rational formula is widely used to estimate either the peak discharges or total discharge volume. In order to make the present analysis compatible with these industry practices, the rational formula is employed to estimate runoff from the urban catchment. The runoff coefficient (f) employed here represents the transformation coefficient of rainfall into runoff, and does not represent the peak discharge coefficient. It is used to obtain the total runoff generated and can be considered as the effective rainfall to be used in a discharge routing model. Continuous simulation is carried out with an appropriately small time step to obtain the outflow hydrograph. As the runoff treated in the present analysis is drained by storm sewers in small sub-catchments, the time of concentration can be very small and may be even lower than the available observation data resolution. The runoff from the catchment is then represented by,

$$\overline{r}_k=\sum_{i=1}^{N}\left(\frac{a_i}{A}\right)r_k f_i \tag{7}$$

where

r_k = generated runoff in mm/Dt at k-th time step
r_k = rainfall at the k-th time step in mm/Δt
Δt = simulation step
A = total catchment area ($\sum a_i$)
a_i = the area of the i-th land use category
N = the number of land use types within the area
f_i = the runoff coefficient for the i-th land use category

A standard two parameter storage function is used to simulate the outflow hydrograph of the catchment. The runoff r given by eq.(7) becomes the input to the storage function model. The storage function model is described by the relationships,

$$Sr=\alpha i^{p} \tag{8}$$

and

$$\frac{dSr}{dt}=\bar{r}-i \tag{9}$$

Equation (8) relates the discharge(i) to the catchment storage Sr through the coefficients a and P. $\bar{r}$ is the inflow available for overland flow. If Manning's law for overland flow is assumed, considering the similarity with the Kinematic wave model, P is taken as 2/3. The catchment runoff described by equation (7) is coupled to the infiltration trenches described by equations(5) and (6), and the basin storage described by equations(8) and (9). The modelling is carried out for individual land use categories and the final outflow hydrograph is obtained by linear superposition. The coupled system is schematically shown in Fig. 3.

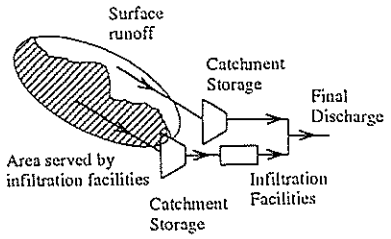

Fig. 3. Schematic diagram of the catchment model with infiltration systems

MODEL APPLICATION

Description of the Observation Site

The Japan Housing and Urban Development Corporation (HUDC) set up a pilot study area in a housing complex in Akishima Tsutsujigaoka Heights, located in the western suburbs of Tokyo, to clarify the problems in a practical application of infiltration systems. The monitoring of storm discharge was carried out at two housing blocks, one of them served by infiltration systems (pilot area), while the other was served by conventional drainage (comparative area). The areas of the pilot and comparative blocks are 1.61 ha and 1.56 ha respectively. The site is equipped with a rain gauge, three flow gauges and 14 tensiometers installed near a trench at 5 to 250 cm depths. The study area is situated on an alluvial upland called the Mushashino platform extending over the west side of Tokyo. The area is covered by a volcanic ash soil called Kanto Loam extending to a depth of 3-4 m. This is underlain by Tachikawa Gravel layer, with a high permeability of around 10^{-2} cm/s. Groundwater is located well below the surface at a depth of 10 m. Outline of the experimental area is shown in Fig.4. The rainfall and discharge measurements at locations G1, G2 and G3 have been carried out at 5 min intervals by automatic recorders.

Soil Properties

The moisture-suction relationship of the Kanto Loam soil was measured from field soil samples and used in the simulation to establish h vs. q/K_0 curves. Saturated conductivity values, measured from small soil samples, were 1.17×10^{-3} cm/s at a depth of 10 cm, 5.8×10^{-4} cm/s at a depth of 130 cm and 9.3×10^{-3} cm/s at a depth of 170 cm. The infiltration trenches are installed at a depth of around 150 cm. Therefore a value of 1.0×10^{-3} cm/s was adopted for K_0 as representative for the whole area. The field moisture-suction curves were measured in the laboratory from undisturbed small soil samples of 5 cm diameter and 5 cm height. These moisture-suction relationships were approximated by the equation.

$$\theta=\frac{\eta(\theta_0-\theta_r)}{\eta+\ln(\varphi)^{\lambda}}+\theta_r \tag{10}$$

where θ = moisture content, θ_0 = saturated moisture content, θ_r= residual moisture content, and η,λ = arbitrary parameters.

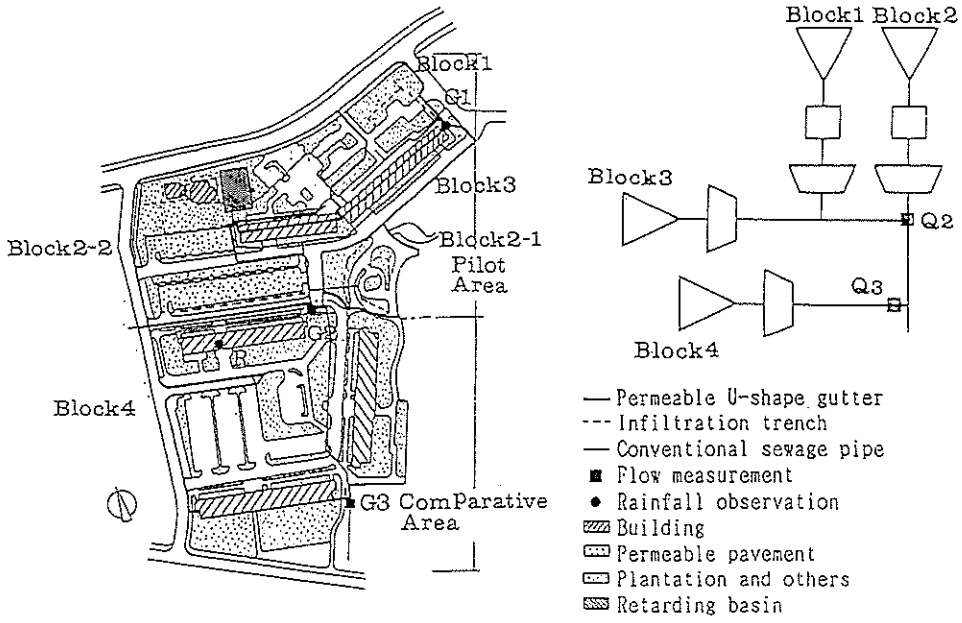

Fig. 4. Outline of the experimental area

The kr(φ) function in eq.(3) is estimated from the θ-φ relation by Mualem's (1978) model given by,

$$kr(\varphi)=\left[\frac{(\theta-\theta_r)}{(\theta_0-\theta_r)}\right]^n \tag{11}$$

TABLE 1 Parameters of measured moisture suction relations

θ_0	θ_r	η	λ
69.76	45.17	51108.1	7.46
78.76	49.33	1841.54	5.24
68.3	43.58	156562	7.46
78.2	50.81	6189.8	5.53

with parameters given in Table 1. A representative θ-φ curve was used for the numerical simulation to establish the infiltration rate-water head relationship given in Fig.2.

Model Parameters

The study area is divided into 4 blocks according to the drainage characteristics, as shown schematically in

Fig. 4. The Blocks nos. 1, 2, and 3 belong to the pilot area, whereas block no. 4 is served by conventional storm drainage. Among the blocks in the pilot area, blocks 1 and 2 are served by infiltration trenches and collection boxes, and all the parking areas in block 2 are made of pervious pavement. Block no. 3 does not have any infiltration facilities even though it belongs to the pilot area. Different land uses and the infiltration facilities in each block are summarized in Table 2.

TABLE 2 Land Use and Infiltration Facility Distribution in the Study Area

Land Use	Block 1	Block 2	Block 3	Block 4	f
Buildings (m^2)	1635.0	803.8	749.2	2711.9	0.95
Roads (m^2)	0.0	368.7	1145.9	4151.6	0.90
Park (m^2)	590.0	2257.5	147.0	0.0	0.90*
Concrete Tiles (m^2)	149.3	1837.0	371.9	1266.9	0.85
Pavement (m^2)	38.0	1173.9	393.0	1159.0	0.70
Greenery (m^2)	110.5	3978.1	303.1	5978.5	0.40
Open Square (m^2)	0.0	32.2	0.0	328.2	0.20
Sand Dump (m^2)	0.0	76.7	0.0	0.0	0.10
Total Area (m^2)	2522.8	10527.9	3110.1	15596.1	
Area with Infiltration Facilities. (m^2)	2374.3	7792.8	0.0	0.0	
Area without Infiltration Facilities. (m^2)	148.5	2735.1	3110.1	15596.1	
f for area with facilities	0.93	0.61	0.0	0.0	
f for area without facilities	0.48	0.13	0.83	0.68	
Length of Trenches (m)	147.50	538.50			
Trench Volume (m^3)	61.95	226.17			

*runoff coefficient of the parks in block 2 was taken as 0.0 to represent pervious pavement

From the h vs. q/K_0 curves in Fig. 1, coefficients 'a' and 'b' in eq.(4), are estimated as, a = 0.008186 and b = 0.000317. The additional parameter required for the simulation is the 'a' value for the storage function model, defined by eqs.(8) and (9). Using one rainfall event, this value was taken as 96 by calibrating against the discharge from block 4, which has no infiltration facilities.

With the above parameters, the model described above was applied for rainfalls with at least 10 mm/hr intensity, recorded between 1989 - 1991 at the site which had continuous records. Figs. 5 and 6 show the hydrographs for the pilot and comparative areas for three representative rainfalls. Each of these figures shows discharges expressed in mm per 5 min. Fig. 7 shows the total computed and observed discharges. From these figures it can be seen that the model performs well for both hydrograph simulation and estimation of total discharges. Table 3 shows the total computed and observed discharges for a number of additional rainfall events.

CONCLUSIONS

Infiltration from trenches and wells occurs as complex saturated-unsaturated flows. These flow characteristics were modelled using linear relations and a model for lumped infiltration systems was produced. The simplified model described was found to be adequate for simulating infiltration system performance at a catchment scale, as both the hydrograph and total volume were well simulated. The effectiveness of infiltration facilities is well demonstrated by reductions in both peak discharge and total runoff volume.

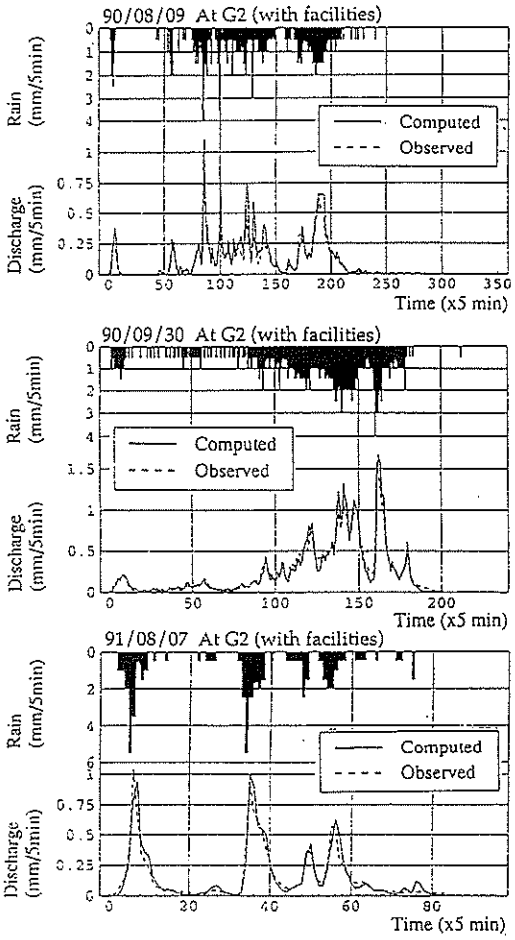

Fig.5. Computed and observed hydrographs for area with infiltration facilities

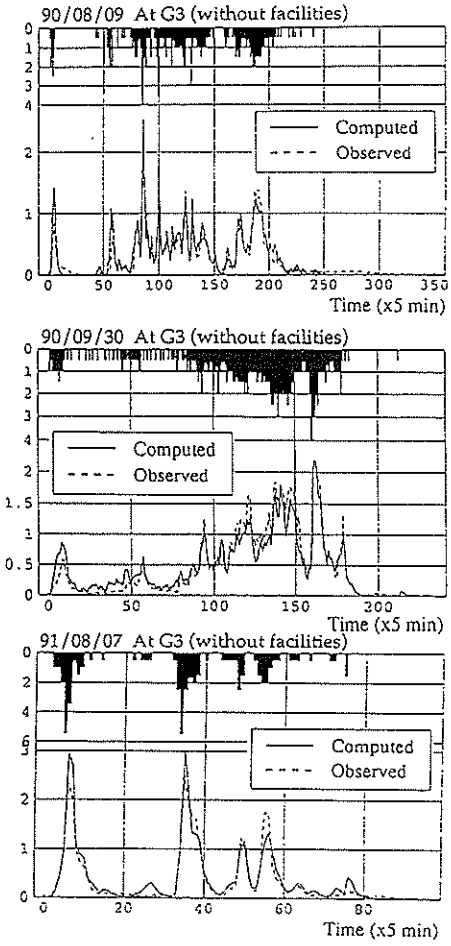

Fig.6. Computed and observed hydrographs for area without infiltration facilities

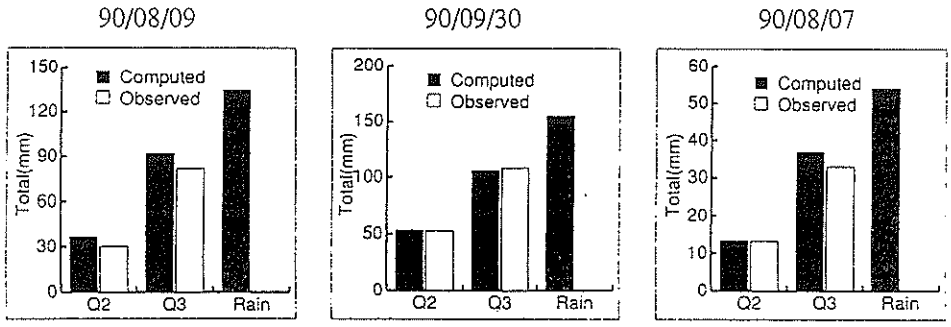

Fig.7. Total discharge volumes (Q2 = area with facilities, G3 = area without facilities)

TABLE 3 Computed and observed total discharge volumes

Date	Q2 (mm) computed	Q2 (mm) observed	Q3 (mm) computed	Q3 (mm) Observed	Rain (mm)
89/08/27	4.42	4.7	12.64	9.88	18.5
89/09/16	13.67	6.48	25.63	17.66	37.5
89/09/20	15.70	8.51	33.83	30.74	49.5
90/08/09	36.33	30.13	91.92	81.70	134.5
90/09/30	53.12	52.70	105.58	108.06	154.5
91/08/07	13.35	13.26	36.90	32.85	54.0
91/08/12	11.24	9.05	23.58	19.63	34.5
91/08/20	15.36	18.60	42.71	50.82	62.5
91/09/13	14.47	9.72	41.00	38.97	60.0

Q2 = Runoff at G2 (with facilities); Q3 = Runoff at G3 (without facilities)

The simple runoff model, described by the effective rainfall and storage function and used in the present study, was adequate for the range of rainfall measurements presently available for the study site. For more complex rainfall and catchment characteristics, the infiltration model described can be coupled to other detailed dynamic runoff models. Unfortunately, due to an equipment malfunction, rainfall events of very high intensities have not been recorded in the past. This has now been corrected and once more data are available, the model will be tested for a wider range of rain events, including the data from other sites.

In modelling infiltration systems, it was assumed that soil initial conditions would not be changed much from the field capacity values. From the tensiometer observations, this assumption is justified as the infiltration takes place about 2 m below the surface, and soil does not become saturated at this depth. It is also noted that small deviations of θ-φ relations do not affect the results much, due to the modelling approach adopted in scaling with respect to soil saturated conductivity. This makes it possible to develop the simplified model represented by eq.(5) and (6) for different types of soils, as well as the infiltration curves given in Fig. 2. Using these graphs and K_0 determined in situ, infiltration systems can be modelled with ease for different locations.

REFERENCES

Herath, S. and Musiake, K. (1987). Analysis of Infiltration Facility performance based on in-situ permeability tests, *Proc. 4th Int. Conference on Urban Storm Drainage*, Lausanne, 61-66.

Herath, S., Musiake, K. and Hironaka, S. (1992). Field estimation of saturated conductivity using borehole test: Effect of unsaturated flow and soil anisotropy, *Proc. Japan Hydraulic Conference*, 435-440.

Mualem, Y. (1978). Hydraulic conductivity of unsaturated porous media: Generalized macroscopic approach, *Water Resources Research*, **14**(2), 325-334.